STELLAR DYNAMO MODELS WITH PROMINENT SURFACE TOROIDAL FIELDS

Alfio Bonanno
INAF—Osservatorio Astrofisico di Catania, via S. Sofia 78, I-95123 Catania, Italy

ABSTRACT

Recent spectro-polarimetric observations of solar-type stars have shown the presence of photospheric magnetic fields with a predominant toroidal component. If the external field is assumed to be current-free it is impossible to explain these observations within the framework of standard mean-field dynamo theory. In this work, it will be shown that if the coronal field of these stars is assumed to be harmonic, the underlying stellar dynamo mechanism can support photospheric magnetic fields with a prominent toroidal component even in the presence of axisymmetric magnetic topologies. In particular, it is argued that the observed increase in the toroidal energy in low-mass fast-rotating stars can be naturally explained with an underlying $\alpha\Omega$ mechanism.

Key words: dynamo – magnetohydrodynamics (MHD) – stars: coronae – stars: magnetic field

1. INTRODUCTION

One of the most compelling problems in modern dynamo theory is the formulation of a realistic coupling between the internal magnetic field and the external field in the atmosphere. In fact, the boundary conditions for the electric and the magnetic field at the stellar surface put severe constraints on the allowed coronal field configurations, and it is often necessary to resort to very crude approximations for the latter.

The standard textbook boundary condition employed in mean-field dynamo theory considers a current-free field in the region $r \geqslant R$, where R is the stellar radius, so that $\nabla \times \boldsymbol{B} = 0$ in this domain. Although in the solar case this assumption is motivated by the possibility of describing the almost rigid rotation of the coronal holes in the lower corona (Nash et al. 1988), it be might incorrect to extend its validity in more active stars.

In fact, as current-free fields represent the states of minimum energy under the constraint that the normal component of the field at the photosphere is fixed, they cannot provide the additional energy required to sustain a significant activity level. Recent measurements of Faraday rotation in the solar corona support the evidence for large-scale coronal currents (Spangler 2007), an essential ingredient to explain coronal heating in terms of Joule dissipation. On the other hand, on much smaller scales, the presence of currents is unavoidable in order to explain the twisted field structure of filaments and prominences.

Force-free magnetic fields, defined by $\nabla \times \boldsymbol{B} = \alpha_{ff}(\boldsymbol{x})\boldsymbol{B}$, where $\alpha_{ff}(\boldsymbol{x})$ is a scalar function, can be more appealing from the physical point of view, at least for very low plasma-β values. However, recent investigations based on direct numerical simulations have shown that the free magnetic energy and the efficiency of coronal heating via current dissipation are still very limited in these models (Peter et al. 2015).

An important consequence of current-free boundary conditions is that the toroidal field must identically vanish in the all domain $r \geqslant R$. In order to illustrate this point in detail, it is convenient to introduce the scalar potential $\Phi(r, \vartheta, \varphi)$ so that the toroidal field can be written as

$$\boldsymbol{B}_{\mathrm{T}} = -\frac{1}{\sin\theta}\frac{\partial\Phi}{\partial\varphi}\boldsymbol{e}_\vartheta + \frac{\partial\Phi}{\partial\vartheta}\boldsymbol{e}_\varphi. \qquad (1)$$

It is not difficult to show that if Φ is a single valued function, $\nabla \times \boldsymbol{B}_{\mathrm{T}} = 0$ in a volume always necessarily implies $\boldsymbol{B}_{\mathrm{T}} \equiv 0$ everywhere (Krause & Raedler 1980). In particular, if the field configuration is spherically symmetric, the azimuthal component of the magnetic field must vanish at the surface, so that $\frac{\partial\Phi}{\partial\vartheta}|_{r=R} = 0$, as imposed in most of the dynamo models (see Moss & Sokoloff 2009 for an interesting discussion on this issue).

Spectropolarimetric observations of photospheric magnetic fields in solar-like stars have revealed surface toroidal field which are mostly axisymmetric and have a predominant toroidal component (Petit et al. 2005, 2008; Fares et al. 2010, 2013; See et al. 2015) implying that most of the magnetic energy resides in the toroidal field. This is the case of the solar-like stars like HD72905, with 82% of the magnetic energy stored in the toroidal field which is nearly completely axisymmetric (97%), or of the G8 dwarf ξ Boo A with 81% of toroidal energy of which 97% is due to the axisymmetric component, or the case of HD56124 with 90% of the energy in axisymmetric field configurations, and roughly the same strength of poloidal and toroidal component. The situation is even more dramatic if one considers M dwarfs like WX UMa or AD Leo where nearly all the energy is stored in an axisymmetric field with prominent photospheric non-zero toroidal component (see See et al. 2015 for a detailed discussion).

While in the case of the Sun a similar observational strategy has confirmed that the magnetic energy is mostly (>90%) poloidal (Vidotto 2016), it is clear that the boundary conditions based on current-free coronal field might not be correct for other, more active stars. In fact, it has been further noticed that fast-rotating, low-mass stars have on average stronger surface toroidal fields than solar-mass slow rotators (See et al. 2016). Can this fact be explained as an enhanced dynamo action due a $\alpha\Omega$ mechanism? Indeed, as strong toroidal fields can alter the average atmospheric structure, there is no reason to assume that a current-free field is still a reasonable approximation for discussing the magnetic energy budget in these objects.

The idea proposed in this Letter is that on large scales and on timescales of the order of the stellar cycle, the external field can be considered harmonic so that

$$\nabla^2\boldsymbol{B} + k^2\boldsymbol{B} = 0, \qquad (2)$$

where the wavenumber k, assumed to be real, determines the characteristic spatial length of the field.

As is well known, in the Sun, various MHD instabilities trigger multiple modes harmonics on different length scales (Nakariakov & Verwichte 2005; Arregui et al. 2013). In more active stars, one can thus argue that the dynamo waves from the interior trigger global oscillations of the coronal field that then propagate according to (2).

It is important to note that linear force-free fields with $\alpha_{ff}^2 = k^2$ are solutions of (2) (note that strictly speaking α_{ff} is a pseudoscalar, while k is a scalar), although the converse is not true in general (Chandrasekhar & Kendall 1957). In this investigation, it turns out that the coronal fields obtained by coupling (2) with dynamo solutions in the interior are approximately force-free in the sense of Warnecke & Brandenburg (2010) as $\langle (\boldsymbol{J} \times \boldsymbol{B})^2 \rangle \ll \langle \boldsymbol{B}^2 \rangle \langle \boldsymbol{J}^2 \rangle$.[1]

It will then be shown that standard MHD continuity conditions at the surface naturally allow for non-zero surface toroidal fields that are directly extrapolated from the interior field produced by the dynamo. In this Letter, several solutions obtained for solar-like stars will therefore be discussed and analyzed. It turns out that depending on the strength of the differential rotation and the surface meridional circulation, it is possible to obtain surface fields whose energies distribution between toroidal and poloidal components is consistent with the observations.

2. BASIC EQUATIONS

Let us assume that the field periodically evolves with a characteristic cycle frequency ω so that $\boldsymbol{B} = e^{-i\omega t}\boldsymbol{\mathcal{B}}$. Equation (2) thus reads

$$(\nabla^2 + k^2)\boldsymbol{\mathcal{B}} = 0, \tag{3}$$

where the wavenumber k is considered to be real. Clearly we must assume that $Rk \ll 1$, otherwise the typical spatial structure of the field would be too short to be consistent with our quasi-homogeneous approximation. As we shall see, as long as $Rk \ll 1$, our results are not quantitatively dependent on the value of k.

As usual, the boundary conditions are the continuity of the normal component of the magnetic field and the tangential component of the electric field across the stellar surface:

$$[[\boldsymbol{n} \cdot \boldsymbol{B}]] = 0, \quad [[\boldsymbol{n} \times \boldsymbol{E}]] = 0, \tag{4}$$

where $\boldsymbol{n}$ is the normal to the surface. In spherical symmetry, the following decomposition for the magnetic field $\boldsymbol{\mathcal{B}}$ can be used

$$\boldsymbol{\mathcal{B}} = -\boldsymbol{r} \times \nabla\Psi - \nabla \times (\boldsymbol{r} \times \nabla\Phi) \equiv \boldsymbol{\mathcal{B}}_{\mathrm{T}} + \boldsymbol{\mathcal{B}}_{\mathrm{P}}, \tag{5}$$

where $\Psi = \Psi(r, \vartheta, \varphi)$ and $\Phi = \Phi(r, \vartheta, \varphi)$ are scalar functions, $\boldsymbol{\mathcal{B}}_{\mathrm{T}}$ is the toroidal component, and $\boldsymbol{\mathcal{B}}_{\mathrm{P}}$ is the poloidal one (see Krause & Raedler 1980 for details). The vector Helmholtz (Equation (3)) decouples in the two scalar equations

$$\nabla^2\Phi + k^2\Phi = 0 \tag{6a}$$

$$\nabla^2\Psi + k^2\Psi = 0 \tag{6b}$$

Table 1
Summary of the Numerical Simulations

$\mathcal{M}$	C_Ω	C_u	$d\Omega/\Omega_{\mathrm{eq}}$	kR	C_α	C_ω	$E_{\mathrm{T}}/E_{\mathrm{tot}}$
A	1000	0	0.1	0.1	7.87	∞	0.67
B	1000	0	0.1	0.4	7.88	∞	0.67
C	1000	0	0.3	0.1	11.24	∞	0.67
D	1000	100	0.3	0.1	7.78	∞	0.37
E	2000	0	0.1	0.1	9.49	∞	0.63
F	2000	0	0.3	0.1	10.97	79.02	0.91
G	2000	0	0.3	vac	11.94	69.98	0
J	4000	0	0.1	0.1	10.11	62.93	0.85
K	4000	0	0.1	0.5	10.04	63.03	0.86
L	4000	100	0.1	0.1	5.57	∞	0.68
M	4000	200	0.1	0.1	5.13	∞	0.37

Note. In particular, it shows how $E_{\mathrm{T}}/E_{\mathrm{tot}}$ depends on C_Ω and various other input parameters ("vac" stands for current-free boundary condition). $\mathcal{M}$ is the model name, and in particular for model J the toroidal and poloidal field are displayed in Figure 1 at various values of the cycle phase.

and variable separation in (6) gives

$$\Phi = R \sum_n^\infty [A_n j_n(\xi x) + B_n y_n(\xi x)] P_n(\cos\theta) \tag{7a}$$

$$\Psi = \sum_n^\infty [C_n j_n(\xi x) + D_n y_n(\xi x)] P_n(\cos\theta), \tag{7b}$$

where x is the normalized stellar radius $x = r/R$, $\xi = kR$, $P_m(\cos\theta)$ are the Legendre polynomials, and $j_n(x)$ and $y_n(x)$ are the spherical Bessel functions. It should be noted that $k = 0$ in (6) does not necessarily imply $\Psi \equiv 0$ in the all $r \geqslant R$ domain, as it must instead hold in the case of a current-free field (vacuum boundary condition).

The A_n–D_n constants are complex numbers whose value must be determined by the boundary conditions (4) imposed at the stellar surface and at some finite outer radius $r = R_{\mathrm{out}}$ where a transition to a wind-dominated field topology occurs (Parker 1958). For our purposes it will be sufficient to assume that at $r = R_{\mathrm{out}}$ the solution is radially dominated so that[2]

$$B_\theta(r = R_{\mathrm{out}}) = B_\phi(r = R_{\mathrm{out}}) = 0. \tag{8}$$

In the stellar interior, the field is described by the mean-field dynamo equation
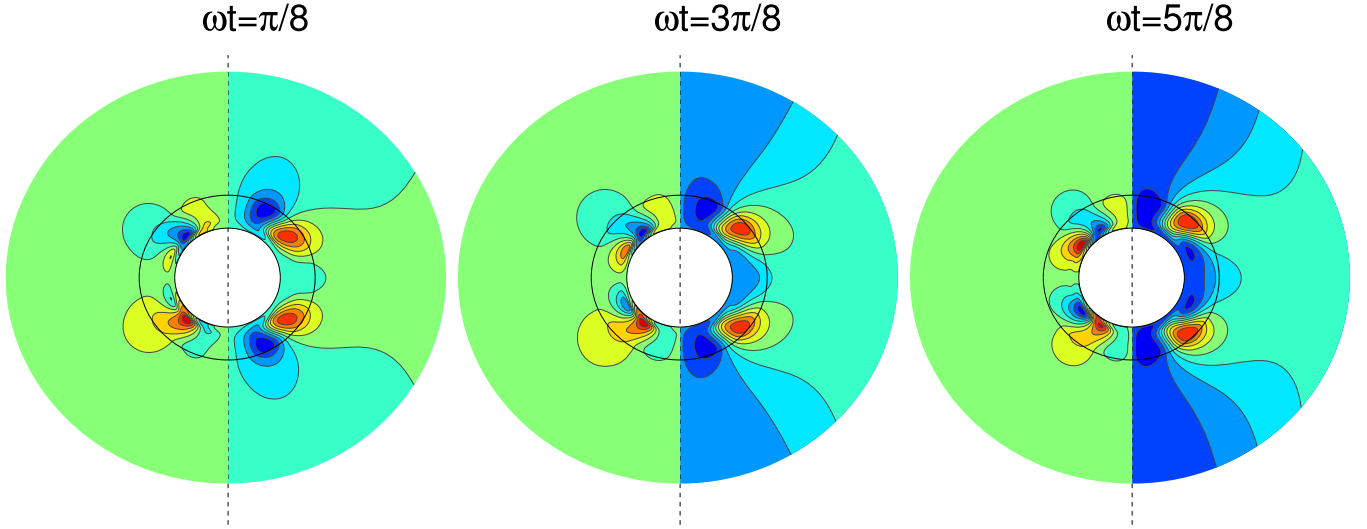
$$\frac{\partial\boldsymbol{B}}{\partial t} = \nabla \times (\boldsymbol{U} \times \boldsymbol{B} + \alpha\boldsymbol{B}) - \nabla \times (\eta\nabla \times \boldsymbol{B}), \tag{9}$$

where, as usual, α is a pseudoscalar function representing the turbulent α-effect, $\boldsymbol{U}$ is the mean flow, and η is the turbulent (eddy) diffusivity. As before $\boldsymbol{B} = e^{-i\omega t}\boldsymbol{\mathcal{B}}$, and we apply the fundamental decomposition (5) for $\boldsymbol{\mathcal{B}}$. Finally, we write

$$\Phi = R \sum_n^\infty \phi_n(x) P_n(\cos\theta) \tag{10a}$$

$$\Psi = \sum_n^\infty \psi_n(x) P_n(\cos\theta), \tag{10b}$$

Figure 1. Temporal evolution of the global (interior+corona) solution for model J of Table 1. The left hemisphere represents the isocontour lines of the toroidal field with blue levels for negative B_φ and red for positive values of the field. The right hemisphere represents the streamlines of the poloidal field. Blue levels are for counterclockwise field lines; red levels for clockwise field lines. Notice the opening of the field lines at $2R$.
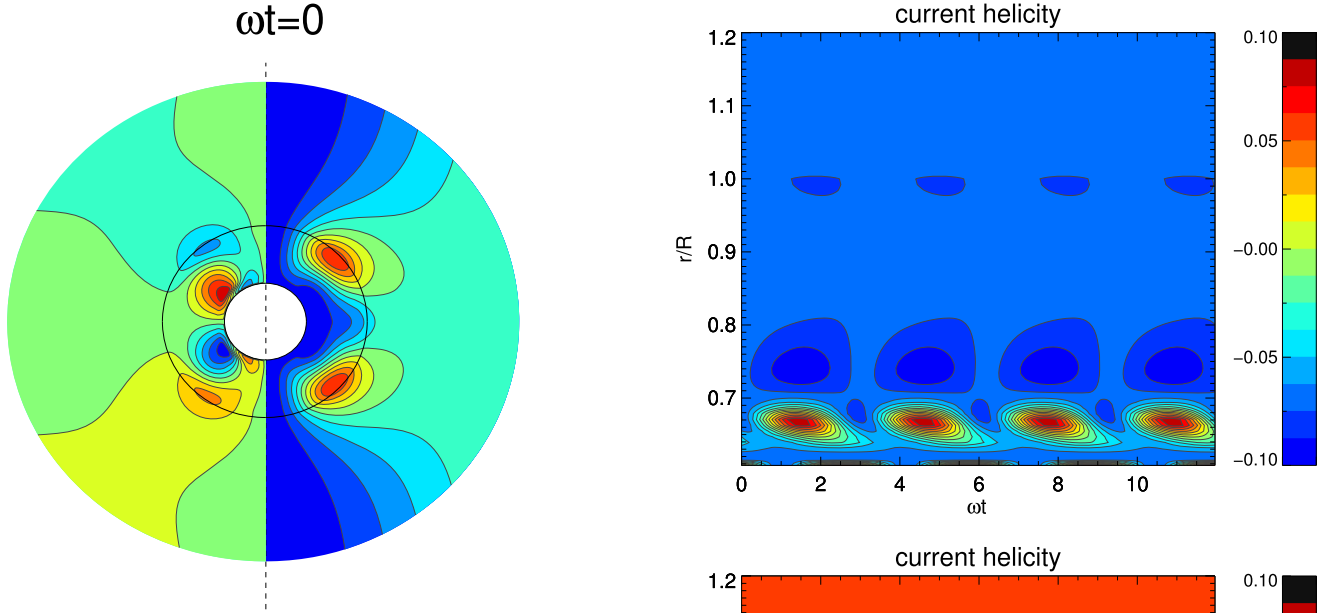
Figure 2. Same as model J, but with a convection zone that extends from $x = 0.5$. In this case, $C_\alpha = 7.86$, $C_\omega = 49.5$, and $E_T/E_{tot} = 0.90$.

where ψ_n and ϕ_n are the complex eigenfunctions of antisymmetric parity of the linear operator (9) (see Rädler 1973 for details).

The field at the inner boundary is assumed to be a perfect conductor, but the boundary conditions (4) at the surface imply the continuity of ϕ_n, ψ_n, and their derivatives across the boundary. It is not difficult to show that in order for the interior solution to be consistent with the external field in (7) the following relation must hold at $x = 1$:

$$\frac{d\phi_n}{dx} + \left[\frac{\gamma_n y_{n+3/2}(\xi) + j_{n+3/2}(\xi)}{\gamma_n y_{n+1/2}(\xi) + j_{n+1/2}(\xi)} - n\right]\phi_n = 0, \qquad (11)$$

where $\gamma_n = A_n/B_n$ are determined by imposing the outer boundary condition (8) on $r = R_{out}$. A similar equation can be obtained for the ψ_n components.

Figure 3. Upper panel: evolution of $\mu_0 R \mathbf{J} \cdot \mathbf{B}/\langle \mathbf{B}^2\rangle$ computed at $+30°$ latitude for an $\alpha^2\Omega$ advection-dominated solar dynamo model with $kR = 0.1$, $C_\alpha = 3.03$, $C_\Omega = 3 \cdot 10^4$, $C_u = 400$, and the cycle period is 32 years. Lower panel: same model as in the upper panel, but the opposite hemisphere. Note that the helicity changes sign from the turbulent zone in the interior to the exterior.

3. DYNAMO MODELS

Let us specialize our formalism to the case of a solar-like star. We assume the following form for the velocity field $U = u(r, \theta) + r \sin\theta \Omega(r, \theta) e_\phi$, and we model the solar-like differential rotation in the following way:

$$\Omega(r, \theta) = \Omega_c + \frac{1}{2}\left[1 + \mathrm{erf}\left(\frac{x - x_c}{d}\right)\right](\Omega_s(\theta) - \Omega_c), \quad (12)$$

where x_c is the location of the convection zone in units of the stellar radius, $d = 0.02$, Ω_c is the uniform angular velocity of the radiative core, $\Omega_s(\theta) = \Omega_0 - d\Omega\cos^2\theta$. Here, $d\Omega = \Omega_{eq} - \Omega_c$ is the surface differential rotation (in principle, obtained from observations). For actual calculations, we fixed $x_c = 0.7$ and $\Omega_c/\Omega_{eq} = 0.9$, but $d\Omega/\Omega_{eq}$ is allowed to vary. The radial profile of the turbulent diffusivity is assumed to be the following:

$$\eta = \eta_c + \frac{1}{2}(\eta_t - \eta_c)\left[1 + \mathrm{erf}\left(\frac{x - x_x}{d}\right)\right], \quad (13)$$

with $\eta_c/\eta_t = 10^{-1}$. The α effect is proportional to $\cos\vartheta$, and its radial profile is assumed to be uniformly distributed in all the convection zone (see Bonanno et al. 2002 for details). The meridional circulation u is obtained from the stream function S (r), which as explained in Bonanno (2013), $S(r)$ can be obtained from an underlying stellar model. The flow as usual is equatorward at the equator and poleward at the surface.

As usual, let us introduce the following dynamo numbers, $C_\Omega = R^2\Omega_0/\eta_t$, $C_\alpha = R\alpha_0/\eta_t$, $C_u = RU_0/\eta_t$, $C_\omega = R^2\omega/\eta_t$, where Ω_0 is the rotation rate at the equator and U_0 is the maximum strength of u_θ at the bottom of the convection zone. The resulting eigenvalue problem can be conveniently solved by inverting a block-diagonal complex matrix (Rädler 1973; Bonanno 2013) that must be truncated to the desired numerical accuracy. For calculations we used the kinematic dynamo code CTDYN, developed by the author, and extensively tested in Jouve et al. (2010). Our results are summarized in Table 1.

Let us first stress that the E_T/E_{tot} at the surface is non-zero, and it is now an increasing function of C_Ω, an effect clearly expected for an $\alpha\Omega$ dynamo. The surface differential rotation also plays an important role because it strongly influences the value of E_T/E_{tot}, as it can be deduced by looking at models E and F, for instance. On the contrary, it should also be noted that E_T/E_{tot} decreased as the flow is increased (see models J, L, and M, for instance). This fact has a clear physical interpretation: as the flow is poleward below the surface, the toroidal belts become more and more confined below the surface at high C_u. It is also reassuring to notice that as long as $kR \ll 1$, our results are not sensitive to the choice of ξ. On the other hand, with the new boundary conditions, the value of the critical C_α is in general smaller than with the standard current-free boundary conditions, as can be observed by looking at models F and G. We also verified that our results are not qualitatively dependent on the location of the external boundary R_{out}. Moreover, low-mass stars with a more extended convection zone have in general higher values of E_T/E_{tot}, if C_Ω is large enough, as discussed in the model of Figure 2.

If the dynamo action is instead driven by the meridional circulation (as in mean-field models of the solar dynamo), the new boundary condition does not alter the internal dynamo action because the toroidal field is localized at the bottom of the convection zone.

In the case of a generic $\alpha\Omega$ advection-dominated dynamo action, we observe a change of sign of the dimensionless ratio $J \cdot B/\langle B^2 \rangle$ from positive (in the northern hemisphere) in the turbulent zone in the interior to negative in the exterior. The opposite happens in the southern hemisphere as one can see in Figure 3. A similar change of sign between the turbulent zone and the exterior has also been observed in Warnecke et al. (2011), although in our mean-field models the current helicity is mostly negative in the outer layers in the northern hemisphere.

4. CONCLUSIONS

The description of the external field in terms of solution of the Helmholtz equation allowed us to extrapolate the internal toroidal field generated by the dynamo on the photosphere, and finally to make contact with the observations. The assumption beyond this idea is the possibility of treating the corona as an external passive medium with effective macroscopic dielectric properties, if averaged over long enough timescales. Although this approach oversimplifies the complex physics of the corona, in our opinion, it represents a significant improvement of the current-free boundary conditions for which $B_T \equiv 0$ on the surface, at least in some classes of very active stars. The resulting dynamo numbers are in general smaller than the standard critical dynamo numbers; the ratio E_T/E_{tot} increases with C_Ω and with a more extended convection zone and decreases with C_u. Indeed, fast-rotating stars with a larger convection zone should approach a cylindrical rotation law in the interior with a smaller surface meridional circulation.

One can therefore argue that the general increase of the surface toroidal energy in low-mass fast-rotating stars finds its natural explanation in an underlying $\alpha\Omega$ dynamo mechanism.

A detailed study of all the parameter space and a comparison with the global topologies inferred from observations will be discussed in a longer paper. We also plan to extend this investigation including non-axisymmetric solutions of higher azimuthal modes.

REFERENCES

Arregui, I., Asensio Ramos, A., & Díaz, A. J. 2013, ApJL, 765, L23
Bonanno, A. 2013, GApFD, 107, 11
Bonanno, A., Elstner, D., Rüdiger, G., & Belvedere, G. 2002, A&A, 390, 673
Chandrasekhar, S., & Kendall, P. C. 1957, ApJ, 126, 457
Fares, R., Donati, J.-F., Moutou, C., et al. 2010, MNRAS, 406, 409
Fares, R., Moutou, C., Donati, J.-F., et al. 2013, MNRAS, 435, 1451
Jouve, L., Brown, B. P., & Brun, A. S. 2010, A&A, 509, A32

Krause, F., & Raedler, K.-H. 1980, Mean-field Magnetohydrodynamics and Dynamo Theory (Oxford: Pergamon)
Moss, D., & Sokoloff, D. 2009, A&A, 497, 829
Nakariakov, V. M., & Verwichte, E. 2005, LRSP, 2, 3
Nash, A. G., Sheeley, N. R., Jr., & Wang, Y.-M. 1988, SoPh, 117, 359
Parker, E. N. 1958, ApJ, 128, 664
Peter, H., Warnecke, J., Chitta, L. P., & Cameron, R. H. 2015, A&A, 584, A68
Petit, P., Dintrans, B., Solanki, S. K., et al. 2008, MNRAS, 388, 80

Petit, P., Donati, J.-F., Aurière, M., et al. 2005, MNRAS, 361, 837
Rädler, K. H. 1973, AN, 294, 213
Reyes-Ruiz, M., & Stepinski, T. F. 1999, A&A, 342, 892
See, V., Jardine, M., Vidotto, A. A., et al. 2015, MNRAS, 453, 4301
See, V., Jardine, M., Vidotto, A. A., et al. 2016, MNRAS, 462, 4442
Spangler, S. R. 2007, ApJ, 670, 841
Vidotto, A. A. 2016, MNRAS, 459, 1533
Warnecke, J., & Brandenburg, A. 2010, A&A, 523, A19
Warnecke, J., Brandenburg, A., & Mitra, D. 2011, A&A, 534, A11